

The hierarchy problem and fine-tuning in a decoupling approach to multi-scale effective potentials

S. Biondini,^{a,1} D. Boer,^{b,2} and R. Peeters^{b,3}

^a*Department of Physics, University of Basel,
Klingelbergstr. 82, CH-4056 Basel, Switzerland*

^b*Van Swinderen Institute for Particle Physics and Gravity,
University of Groningen, NL-9747 AG Groningen, The Netherlands*

Abstract: In many realizations of beyond the Standard Model theories, new massive particles are introduced, leading to a multi-scale system with widely separated energy scales. In this setting the effective potential, which takes into account quantum corrections for the scalar sector, has to be supplemented with a prescription to handle the hierarchy in mass scales. In this paper, we focus on the so-called decoupling method, which freezes the effects of heavy particles on the RG running of the light degrees of freedom at low energies. For a two-scalar theory, we disentangle the effects of the high-energy degrees of freedom on the shape of the potential and on the fine-tuning of the model parameters. We find that, while the decoupling method leads to an acceptable and convergent effective potential, the method does not solve the fine-tuning problem that is inherent to the hierarchy problem of multi-scale theories. We also consider two alternative implementations of the decoupling, which give different results for the shape of the potential, but still lead to similar conclusions on the amount of fine-tuning in the model.

¹simone.biondini@unibas.ch

²d.boer@rug.nl

³r.j.c.peeters@rug.nl

1 Introduction

The Standard Model (SM) of particle physics is our present-day reference for a detailed understanding and description of the fundamental building blocks of matter and the interactions among them. Despite its success, some new physics is expected because of various compelling observations and measurements that still require clarification, such as the nature and generation of neutrino masses, the hierarchies among fermion masses, the nature of dark matter, the baryon asymmetry in the universe and the origin of electroweak symmetry breaking. The current view of the SM, which has developed over the past few decades, is that of an effective low-energy theory of some unknown ultraviolet (UV) completion.

If the theory that extends the SM is meant to solve one of the aforementioned open questions, it is likely that new degrees of freedom couple with the SM particles. The Higgs sector is especially interesting in this regard, as the Standard Model Higgs boson is often taken as a portal between the visible and a dark sector [1–4], it enters the interactions with right-handed neutrinos in the leptogenesis framework to account for the baryon asymmetry [5], and the origin of the electroweak symmetry breaking could be explained if the Higgs couples to additional scalar particles [6–9]. However, the existence of interactions between the Higgs boson and any heavier state of new physics comes at the price of generating quantum corrections to the Higgs mass that are quadratic in the mass of the heavy particle [10–14]. These corrections cannot be avoided on the basis of symmetry arguments [12], and make the Higgs mass extremely sensitive to high-scale physics. In light of the absence of new-physics signatures at the TeV scale, the observed Higgs mass appears rather “unnatural”, as quadratic corrections would involve increasingly higher energy scales [15]. This constitutes the so-called *hierarchy problem*: how to explain why the electroweak scale is so small if there is any beyond the Standard Model physics at high scales.⁴

The hierarchy problem can also be viewed as a fine-tuning problem, as the parameters of new high-scale physics have to be chosen very carefully in order to result in the observed low-energy parameters. Besides the vacuum energy density, this effect is most pronounced in the mass parameter, which receives large corrections in the renormalization group (RG) running from high to low energies, especially when there is a large hierarchy between the different scales. There are some well-known theories that address the hierarchy problem at the TeV scale, like supersymmetric extensions [17–20], composite Higgs [21–23] and extra dimensions [24–26]. However the minimal versions of these models are nowadays rather fine-tuned in order to stay compatible with experiments [15, 27–29].

In this paper we do not consider specific theories that aim to solve the hierarchy problem, but will take a closer look at various aspects of the hierarchy problem from the perspective of the effective potential.⁵ This is the proper quantity to determine the true minimum of a scalar field

⁴If one treats the electroweak and gravitational forces within the same quantum field theory framework, then quantum-gravity loop corrections to the Higgs mass must be included as well. However, one may argue that the Planck mass defines an interaction scale rather than a new particle’s mass scale, see e.g. ref. [16].

⁵See ref. [30] for an extensive review of the effective potential both at zero and finite temperature.

theory and its stability at the quantum level. In addition, it allows to quantitatively address the effect of including loop corrections on the properties of scalar particles (masses, couplings, vacuum expectation values). Here, we are especially interested in the scenario where there is a large hierarchy of mass scales in the model, so as to resemble a high-energy extension of the Standard Model. When new mass scales are introduced, the sensitivity of the low-energy parameters to the high-energy UV physics is reflected in different observables obtained from the effective potential, such as the vacuum expectation value (VEV) and mass of the low-energy scalar field.

There is, however, an additional difficulty when a multi-scale effective potential is considered. The loop expansion of the effective potential contains logarithms of the ratio m_i^2/μ^2 , with m_i being the mass eigenvalues of the model, and μ the renormalization scale. In a model with a hierarchy in mass scales, it is impossible to choose a value for μ such that all logarithms containing the ratio m_i^2/μ^2 are small at the same time. The remaining large logarithms will appear with higher powers at higher orders, invalidating the loop expansion. The non-convergence of the perturbative expansion of the effective potential in the presence of a multi-scale system will hamper its predictiveness. At the level of the effective potential, various approaches to handling a multi-scale system have been put forward: (i) multi-scale renormalization methods [31–33]; (ii) a decoupling method in mass-independent renormalization schemes [34–36]; (iii) a more recent implementation via a single-scale renormalization-group improvement for multi-scale effective potentials [37]. In ref. [36] it was shown within the Higgs-Yukawa model that the decoupling method is equivalent to the multi-scale method used in [32, 33]. Conversely, the single-scale improvement is not equivalent to the other two methods, as it does not always resum the leading logarithms [37]. For these reasons, we choose to focus on the decoupling method of [36] in this paper. We will also comment on two other methods: first a more general implementation of the decoupling prescription [38] and then a method using effective field theory (EFT) techniques [39, 40].⁶

Here, we consider a rather simple model with two scalar fields, where we take the mass parameters with a large scale separation. Moreover, the light scalar field undergoes spontaneous symmetry breaking (SSB) at tree-level, whereas the additional heavy scalar field, that mimics the new physics, does not (see refs. [38, 39] for a similar model). The two-scalar model comprises the main ingredients to inspect fully the hierarchy problem and it may resemble the Standard Model Higgs sector extended with an unknown high-energy completion. Our goal is to address two main aspects of the hierarchy problem when implementing the decoupling approach: (i) checking whether the SSB still occurs at the quantum level in the presence of high-energy degrees of freedom, and to which extent the minimum of the potential and the mass of the light scalar are affected; (ii) inspecting the fine-tuning of the model parameters. To the best of our knowledge, these two issues have not been discussed in detail in the framework of the effective

⁶The latter reference [40] reproduces the decoupling prescription for the Higgs-Yukawa model, though the derivation is more rigorous.

potential in a scenario with well-separated mass scales. We shall compare the results of the standard implementation of the effective potential with the decoupling prescription for handling a multi-scale system.

The paper is organized as follows. In Sec. 2 we introduce the two-scalar model and highlight the different aspects of the hierarchy problem in the context of the effective potential. Then in Sec. 3, after the decoupling method is introduced, we address the numerical evaluation of the VEV of the low-energy scalar field, its stability under radiative corrections and its mass in Sec. 3.1, while in Sec. 3.2 the connection between fine-tuning and the effective potential is studied. In Sec. 4 we elucidate different implementations of the decoupling method, one of which is an EFT approach for handling the effects of heavy degrees of freedom on the effective potential. Finally, the conclusions are offered in Sec. 5.

2 A large hierarchy in the effective potential

In order to set a reference for the decoupling approach, we discuss the different problems that appear when we naively apply the effective potential formalism to a theory with a hierarchy in the mass parameters (referred to as the non-decoupling approach). To this end, we work with a simple model, which is a theory with two real scalar particles. The model Lagrangian can be written as follows:

$$\mathcal{L} = \frac{1}{2}\partial_\mu\phi\partial^\mu\phi + \frac{1}{2}\partial_\mu S\partial^\mu S - V(\phi, S), \quad (2.1)$$

where the potential with bare parameters reads

$$V(\phi, S) = \frac{1}{2}\mu_\phi^2\phi^2 + \frac{1}{2}\mu_S^2 S^2 + \frac{\lambda_\phi}{4}\phi^4 + \frac{\lambda_S}{4}S^4 + \alpha\phi^2 S^2. \quad (2.2)$$

On the one hand, the parameters of the field ϕ are chosen to achieve spontaneous symmetry breaking at tree level, so we take $\mu_\phi^2 < 0$ with the corresponding VEV $v_\phi = \pm\sqrt{-\mu_\phi^2/\lambda_\phi}$. On the other hand, the mass parameter for the S field already corresponds to a physical mass and we take it to satisfy $\mu_S^2 \gg |\mu_\phi^2|$. As mentioned, the scalar field S plays the role of a high-energy degree of freedom and it belongs to the UV energy domain in our model (the highest scale we shall consider when running the parameters will be μ_S). We remark that the heavy field does not develop a VEV. This will still hold under radiative corrections to the heavy scalar mass, since the corrections from both μ_S and μ_ϕ are not large enough to flip the sign of μ_S^2 . To ensure that the potential Eq. (2.2) is bounded from below, there are some constraints on the quartic couplings (see e.g. ref. [41]):

$$\lambda_\phi > 0, \quad \lambda_S > 0, \quad \alpha > -\frac{1}{2}\sqrt{\lambda_\phi\lambda_S}. \quad (2.3)$$

Next we turn to the effective potential for the model. The RG-improved effective potential in any mass-independent renormalization scheme can be organized in a loop expansion $V_{\text{eff}} =$

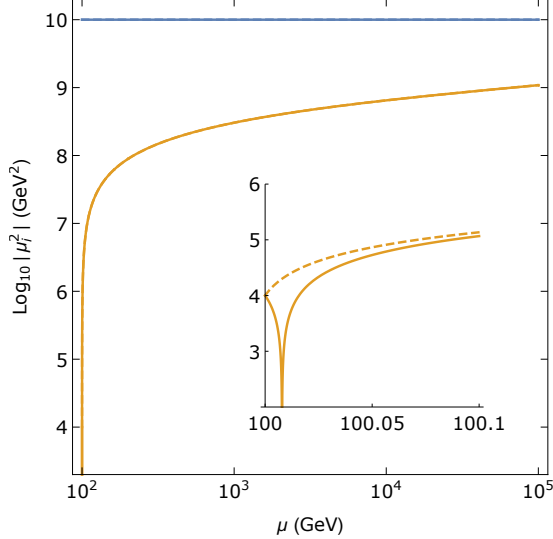


Figure 1: The RG running of the mass parameter μ_ϕ^2 (orange) at 1-loop level using the benchmark point described in the text, with $\alpha > 0$ (solid line) and $\alpha < 0$ (dashed line). The value of μ_S^2 is constant (solid blue), as explained in the text.

$V^{(0)} + V^{(1)} + \dots$, where $V^{(0)}$ is the RG-improved tree-level potential and $V^{(1)}$ is the one-loop correction after renormalization which reads (using the $\overline{\text{MS}}$ scheme):

$$V^{(1)} = \frac{1}{4(4\pi)^2} \left\{ m_\phi^4 \left[\log \frac{m_\phi^2}{\mu^2} - \frac{3}{2} \right] + m_S^4 \left[\log \frac{m_S^2}{\mu^2} - \frac{3}{2} \right] \right\}. \quad (2.4)$$

The masses in this expression are the tree-level masses, as a function of the classical field value ϕ_c . They are found to be

$$m_\phi^2 = \mu_\phi^2 + 3\lambda_\phi \phi_c^2, \quad m_S^2 = \mu_S^2 + 2\alpha \phi_c^2. \quad (2.5)$$

According to our assumptions, the heavy scalar does not develop a nonzero VEV by construction, so that we can set $S_c = 0$. Therefore, the masses in Eq. (2.5) are independent of S_c . When extracting the counterterms of the effective potential, one can see that μ_S^2 , λ_S and α do not run, in contrast to λ_ϕ and μ_ϕ^2 . The resulting β -functions for λ_ϕ and μ_ϕ^2 are given by:⁷

$$\beta_{\lambda_\phi} = \mu \frac{\partial \lambda_\phi}{\partial \mu} = \frac{1}{8\pi^2} (9\lambda_\phi^2 + 4\alpha^2), \quad (2.6)$$

$$\beta_{\mu_\phi^2} = \mu \frac{\partial \mu_\phi^2}{\partial \mu} = \frac{1}{8\pi^2} (3\lambda_\phi \mu_\phi^2 + 2\alpha \mu_S^2). \quad (2.7)$$

⁷We checked that, when letting S_c have a varying field value, we recover the full set of RGEs, see e.g. ref. [42].

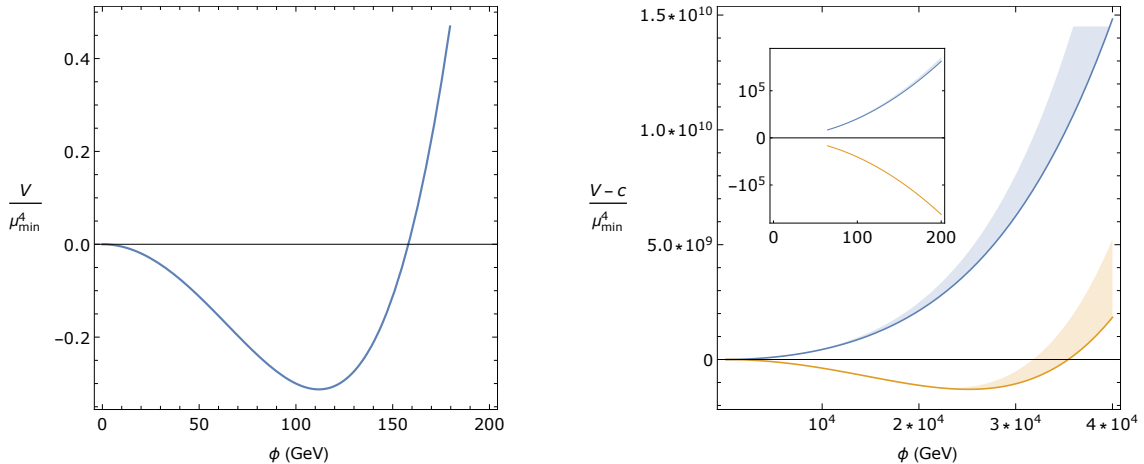


Figure 2: The shape of the scalar potential in the non-decoupling case. The left figure shows the tree-level result, evaluated at $\mu = \mu_{\min}$. The right plot shows the results including the 1-loop contributions for $\alpha > 0$ (blue solid line) and $\alpha < 0$ (orange solid line). In the right figure, a constant term c is subtracted as explained in the text to normalize the potential to zero at $\phi = 0$. The solid lines in the right plot show the result for $\mu = \mu_{\min}$, and a band is shown for the range $\mu_{\min} \leq \mu \leq \mu_{\max}$.

In order to illustrate the behaviour of this model, we will use a benchmark point for the parameter space throughout the paper. The parameter values are:

$$\begin{aligned} \mu_\phi^2(\mu_{\min}) &= -(10^2 \text{ GeV})^2, & \mu_S^2(\mu_{\min}) &= (10^5 \text{ GeV})^2, \\ \lambda_\phi(\mu_{\min}) &= 0.8, & \lambda_S(\mu_{\min}) &= 1.3, & \alpha(\mu_{\min}) &= \pm 0.5. \end{aligned} \quad (2.8)$$

where $\mu_{\min} = 100 \text{ GeV}$. Furthermore, we take μ_S as the maximum value for the renormalization scale, so $\mu_{\max} = 10^5 \text{ GeV}$. As we will see, changing the sign of α has a large effect on some of the results. Hence, we will use both a positive and negative value for α in our benchmark point. We adopt this set of parameters for all numerical results presented in our paper, unless explicitly stated otherwise. The running of the mass parameter μ_ϕ^2 (and the comparison with the constant μ_S^2) in this model is shown in Fig. 1. One observes that μ_ϕ^2 receives large corrections from the high-energy modes already for small deviations from the initial renormalization scale. This is an expression of the hierarchy problem. When $\alpha > 0$, the μ_S^2 contributions to the running of μ_ϕ^2 are positive, and μ_ϕ^2 flips sign already at $\mu = 100.008 \text{ GeV}$ (solid orange line). At high energy a large positive value of $\mu_\phi^2 \approx 10^9 \text{ GeV}$ is reached. For $\alpha < 0$, there are only negative contributions to the running of μ_ϕ^2 . So the value at high energy will have the opposite sign as in the case $\alpha > 0$, but the absolute value is essentially the same, since the small initial value of μ_ϕ^2 at μ_{\min} has practically no effect on the high-energy value. Therefore, in the following we will often select only a particular sign of α to illustrate some point.

2.1 Properties of the light scalar from the effective potential

In this section we address the shape of the potential and the corresponding mass eigenvalue of the scalar field ϕ when we include the 1-loop corrections. Let us begin with the study of the shape of the potential for different values of the renormalization scale, and for both $\alpha > 0$ and $\alpha < 0$, that we show in Fig. 2. The left plot shows the tree-level result evaluated at the scale μ_{\min} . This potential exhibits the well-known Mexican-hat behaviour. In the right plot, the 1-loop contributions are added and the behaviour is quite different from the tree-level result. First of all, as can be seen from eqs. (2.4) and (2.5), there is a large constant term present in the potential ($\propto \mu_S^4$), which leads to a shift in the potential. In order to normalize the potential to zero at $\phi = 0$, and better compare the shape of the potential with the tree-level case, we subtract from the one-loop potential the following term

$$c = \frac{\mu_S^4}{64\pi^2} \left(\log \frac{\mu_S^2}{\mu^2} - \frac{3}{2} \right) + \frac{\mu_\phi^4}{64\pi^2} \left(\log \frac{\mu_\phi^2}{\mu^2} - \frac{3}{2} \right). \quad (2.9)$$

We note that the μ_ϕ^4 term in Eq. (2.9) is always subdominant. However, for large μ values it does give a sizable contribution as in that case μ_ϕ^2 is only an order of magnitude smaller than μ_S^2 (see Fig. 1). Looking at the shape of the potential, there is a clear difference between $\alpha > 0$ and $\alpha < 0$. When $\alpha > 0$, there is no non-trivial minimum anymore, hence no spontaneous symmetry breaking can occur (solid blue line). This happens because the contributions proportional to m_S^4 dominate the potential, and they are all positive (recall the expression for m_S^2 in Eq. (2.5)). In the case $\alpha < 0$, the m_S^4 term in the potential gives both positive ($\alpha^2\phi^4$) and negative ($\alpha\mu_S^2\phi^2$) contributions. The competition between these terms results again in a Mexican-hat shape, as can be seen in the right panel of Fig. 2 (solid orange line). However, the location of the VEV is very different from the tree-level case, with a value for the 1-loop VEV of $v_\phi^{(1)} \approx 2.5 \cdot 10^4$ GeV much larger than the tree-level VEV $v_\phi^{(0)} \approx 112$ GeV. In the figure, a band is shown for the range $\mu_{\min} \leq \mu \leq \mu_{\max}$ which demonstrates that the results are largely independent of the chosen scale. We also note that for small values of $\phi = \phi_c$, both lines stop, which happens because of the appearance of imaginary values of the potential. This is a well-known feature that does not imply a breakdown of the effective potential approach, but rather signals a decaying state. For details we refer to [43].

Next, we want to see the effect of the 1-loop contributions on the mass of the light boson, as this is important in understanding the hierarchy problem in this model. In general, the mass of ϕ is given by the second derivative of the potential with respect to ϕ . The full expression contains the tree-level contribution and 1-loop contributions from the ϕ and S sectors. We single out the dominant term, which is the one that depends on the heavy scale μ_S^2 :

$$m_\phi^{2,(1)}(\mu) \sim \frac{\alpha}{16\pi^2} (\mu_S^2 + 2\alpha\phi_c^2) \left[\log \frac{\mu_S^2 + 2\alpha\phi_c^2}{\mu^2} - 1 \right]. \quad (2.10)$$

For $\mu \not\approx e^{-1/2}m_S$, this term is large and pushes the mass of ϕ to large values. Notably, there is

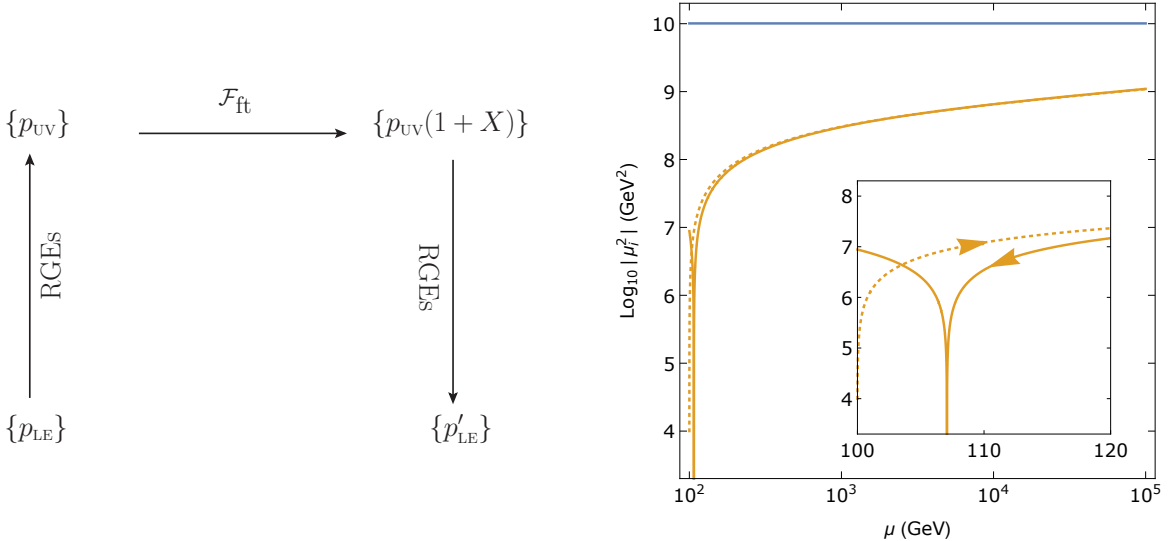


Figure 3: (Left) Diagrammatic representation of the prescription for determining the amount of fine-tuning (p_{LE} and p_{UV} stand for the parameters at low-energy and at the ultraviolet scale respectively). There is running of the parameters from low to high energy, a shift of the parameters through \mathcal{F}_{ft} and running back to low energy. (Right) The result of running the mass parameters up from low energy (dotted line) and down from high energy after changing the high-energy parameters with $X = 0.01$ (solid line), with $\alpha < 0$.

a large shift in m_ϕ^2 already for $\mu = \mu_{min}$. This is how the hierarchy problem of the Higgs mass manifests itself in this model.

Finally, we want to make contact between the effective potential and the amount of fine-tuning that is necessary at high energy (μ_{max}) in order to obtain a small value for μ_ϕ^2 at low energy (μ_{min}). To this end, we start with the model defined at the initial scale μ_{min} . Then, we run the parameters up to the high-energy scale μ_{max} using the RG equations (2.6) and (2.7). Here, we implement a variation by multiplying the parameters with $\mathcal{F}_{ft} = 1 + X$, with $X \in [0, 1]$, and then run the parameters back down to μ_{min} . A diagrammatic representation of the prescription is given in Fig. 3 (left). An example of the μ_ϕ^2 -running from high energy down to low energy, after a variation at high energy is implemented, is shown in Fig. 3 (right). With only a 1%-level variation at the high-energy scale, we see that the low-energy value of μ_ϕ^2 shifts from -10^4 GeV² to -10^7 GeV². Hence, a small variation at the high scale has an enormous effect at low energy. This indicates that in order to obtain the desired low-energy value for μ_ϕ^2 , a large amount of fine-tuning is necessary.

Let us summarize the findings so far. The effective potential has been used to study the shape of the potential, the VEV of the low-energy field ϕ , the mass of ϕ and the fine-tuning of the model parameters. As for the features related to the shape of the potential, we see that the

effect of including the 1-loop corrections is large. Even at the scale $\mu = \mu_{\min}$ there are large corrections to the location of the VEV and the mass of the light scalar. For the fine-tuning we see that already for small deviations from the initial scale μ_{\min} , the high-energy degrees of freedom are active and provide large radiative corrections. The high-scale theory therefore needs a large amount of fine-tuning in order to accommodate the large hierarchy at low energy.

As mentioned in the introduction, the perturbative expansion of the effective potential will involve large logarithms when a large hierarchy in scales is present. As can be seen from the expression for the 1-loop potential in Eq. (2.4), ratios of scales appear in the two logarithms: m_ϕ^2/μ^2 and m_S^2/μ^2 with $m_\phi^2 \ll m_S^2$. Because of this hierarchy it is not possible to find a value of μ such that both logarithms in Eq. (2.4) are small at the same time. This problem invalidates the loop expansion, because such logarithms will appear with higher powers at higher orders. The non-convergence of the perturbative expansion of the effective potential in the presence of a multi-scale system hampers its predictiveness. The decoupling method has been proposed as a possible solution to this problem and in the next section we will quantitatively study this approach.

3 The decoupling method

The main idea behind the decoupling method is to decouple *by hand* any particle in the theory as soon as the energy is too low to excite its modes [34–36]. In practice, one introduces step functions in the effective potential, such that the contribution of particles with a mass larger than the decoupling scale μ_{dec} is switched off. Using this prescription, the full effective potential can be safely evaluated down to the energy scale of the lightest particle. For the model at hand, the one-loop contribution can then be written as follows

$$V_{\text{dec}}^{(1)} = \frac{1}{4(4\pi)^2} \left\{ \theta(\tilde{\mu} - m_\phi) m_\phi^4 \log \frac{m_\phi^2}{\tilde{\mu}^2} + \theta(\tilde{\mu} - m_S) m_S^4 \log \frac{m_S^2}{\tilde{\mu}^2} \right\}, \quad (3.1)$$

where we write $\tilde{\mu}^2 = \mu^2 e^{3/2}$, in order to absorb the usual numerical factor, which is 3/2 for scalars. We can determine the β -functions by taking the derivative with respect to the renormalization scale μ of $V_{\text{dec}}^{(1)}$.⁸ In order to avoid some clutter, we define $\theta_i \equiv \theta(\tilde{\mu} - m_i)$. The decoupling is inherited by the two parameters λ_ϕ and μ_ϕ^2 so that the β -functions now read:

$$\beta_{\lambda_\phi} = \mu \frac{\partial \lambda_\phi}{\partial \mu} = \frac{1}{8\pi^2} (9\lambda_\phi^2 \theta_\phi + 4\alpha^2 \theta_S), \quad (3.2)$$

$$\beta_{\mu_\phi^2} = \mu \frac{\partial \mu_\phi^2}{\partial \mu} = \frac{1}{8\pi^2} (3\lambda_\phi \mu_\phi^2 \theta_\phi + 2\alpha \mu_S^2 \theta_S). \quad (3.3)$$

⁸We note that the step functions do not contribute to this derivative, since they give a factor $m_i^4 \delta(\tilde{\mu} - m_i) \log \frac{m_i^2}{\tilde{\mu}^2}$. This factor is always zero, because for the single value where the δ -function is non-zero, the logarithm vanishes. Also note that one could replace the step functions by smooth versions, but this will not affect our conclusions.

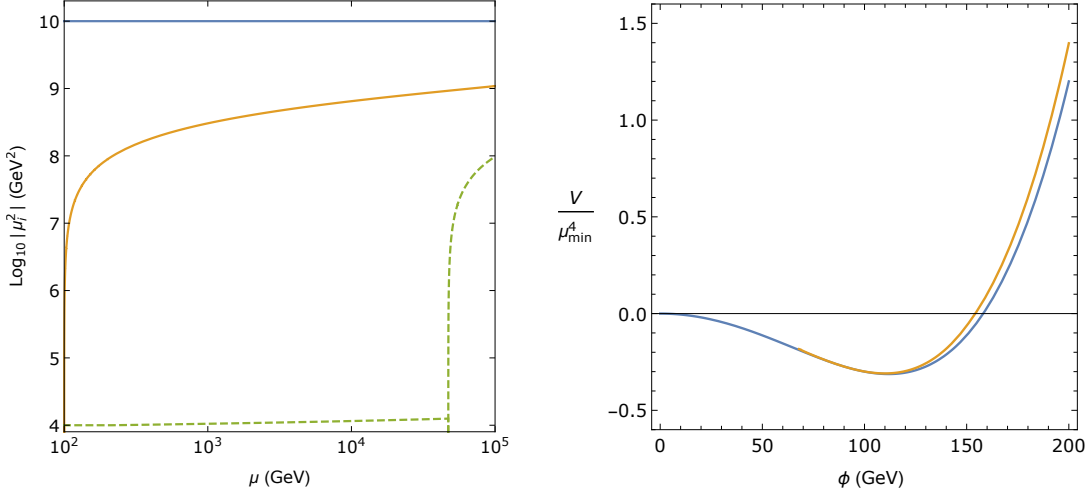


Figure 4: (Left) The running of the mass parameters, with μ_S^2 in blue, and μ_ϕ^2 in solid orange for the case without decoupling, and in dashed green for the case with decoupling, using $\alpha > 0$. (Right) A comparison between the shape of the tree-level potential evaluated at $\mu = \mu_{\min}$ (blue line) and the tree-level + 1-loop potential using the decoupling method (orange line). The potential is plotted in units of V/μ_{\min}^4 .

In our setting, when we run down from high energy, we obtain first a decoupling of the heavy S field. For $\tilde{\mu} < m_S$, i.e. $\mu \approx \mu_{\max}/2$, the effect of the heavy degree of freedom on the running parameters is absent and the change with the renormalization scale is only due to the lighter scalar ϕ . Going further down $\tilde{\mu} < m_\phi$, the couplings are frozen and do not run anymore. So the decoupling method provides a prescription for the renormalization scale μ [36], which is setting it equal to or smaller than the lowest decoupling scale $\mu^* \equiv m_\phi e^{-3/4}$ (which in our setting we take anyway larger than μ_{\min}). In this way, the loop contributions are absent, so the problematic logarithms disappear from the potential. Only the RG-improved tree-level contribution $V^{(0)}(\mu < \mu^*)$ remains. This prescription ensures that higher-loop contributions also vanish, restoring the predictivity of the perturbative expansion.⁹

In Fig. 4 (left) one finds the mass parameter μ_ϕ^2 evolved with and without decoupling, in order to show the strongly different behaviour. The same benchmark point is used as in the case without decoupling, with $\alpha > 0$. This figure shows that when using the decoupling method, μ_ϕ^2 remains small for most of the considered energy range since the high-energy modes only start contributing at $\mu \approx \mu_{\max}/2$. Moreover, although the high-energy modes do contribute to the RG running for $\tilde{\mu} > m_S$, the final value of μ_ϕ^2 at μ_{\max} is one order of magnitude lower than in the case without decoupling. The results are essentially the same for $\alpha < 0$, even though it

⁹In order to find an appropriate renormalization scale, the authors of ref. [36] suggested two conditions: $V_{\text{dec}}^{(1)}(\mu) = 0$ (best perturbative convergence) and $d(V^0 + V_{\text{dec}}^{(1)})/d\mu = 0$ (least μ -dependence). When choosing the renormalization scale smaller than the smallest mass eigenvalues, the two prescriptions are fully equivalent.

changes the value of m_S (cf. Eq. (2.5)) and therefore the value of the decoupling scale. This effect will be small, because we only consider small values for ϕ_c , so it will not change the fact that the high-scale modes contribute above $\mu \approx \mu_{\max}/2$.

3.1 Minimum and shape of the potential

Let us now use the prescription for the renormalization scale in the decoupling method to evaluate the effective potential. A comparison between the tree-level result and the one-loop result in the decoupling method is shown in Fig. 4 (right). It is worth stressing that the shape of the 1-loop effective potential (solid-orange line in Fig. 4) is independent of the sign of α (whereas this affects severely the 1-loop effective potential in the naive implementation, see Fig. 2). This is due to the absence of α -dependent terms at scales $\tilde{\mu} < m_S$. In contrast to the case without decoupling, we now see that the 1-loop effective potential only introduces small corrections, signalling a good perturbative expansion at least in the low-energy domain and at this loop order. Moreover, one can see that a non-trivial minimum is realized and spontaneous symmetry breaking can occur, also for $\alpha > 0$. The truncation of the orange solid line is due to the squared mass eigenvalue m_ϕ^2 turning negative for values $\phi_c \leq 68$ GeV for this choice of the parameters. This makes it impossible to define a meaningful decoupling scale, and leads to the aforementioned decaying state [43], but we will not address this further here.

We have checked numerically that the good agreement between the tree-level potential and the decoupling potential is not due to the specific choice of parameters in the benchmark point. For different low-energy values of λ_ϕ and μ_ϕ^2 , the shift in the value of the VEV $v^{(1)}$ is at the few-percent level.

Let us now look at what happens to the mass of the ϕ scalar when the decoupling method is used. Since the 1-loop contributions are absent from the potential in this case ($V_{\text{dec}}^{(1)} = 0$), the term that previously pushed m_ϕ to large values no longer contributes. The mass of the ϕ boson is now given by:

$$m_\phi^2(\mu < \mu^*) = \mu_\phi^2 + 3\lambda_\phi\phi_c^2, \quad (3.4)$$

where all parameters are understood to be evaluated at the same scale $\mu < \mu^*$. In contrast to Eq. (2.10), there are no μ_S^2 contributions in Eq. (3.4), and the decoupling method ensures the lightness of the ϕ boson.

3.2 Fine-tuning

In this section we repeat the fine-tuning analysis carried out in Sec. 2 for the decoupling approach. In contrast to Sec. 3.1, the whole range of energy scales is now directly involved, since we have to use the RGEs up to the high-energy domain. Accordingly, above the decoupling value $\tilde{\mu} > m_S$, the heavy degree of freedom is active and affects the running considerably. We use the same procedure as in the case without decoupling, where we run the low-energy parameters up to the

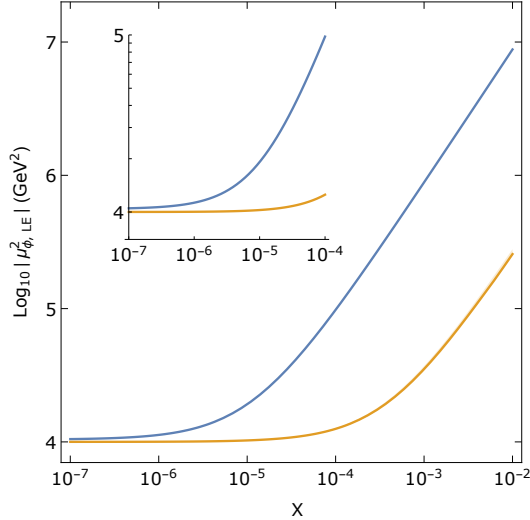


Figure 5: The effect of small variations in the high-energy value of the parameters on the low-energy value $\mu_{\phi, \text{LE}}^2 = \mu_{\phi}^2(\mu_{\text{min}})$, using the benchmark point with $\alpha > 0$. The results for the decoupling (orange line) and non-decoupling (blue line) cases are compared. A field value of $\phi_c = 300$ GeV is used.

high scale, then vary them at the high scale, and run them down to low scale. In this case we use the RGEs (3.2) and (3.3) that govern the decoupling.

In order to compare the sensitivity to the high-energy parameters with and without the decoupling prescription, we show in Fig. 5 the value of μ_{ϕ}^2 evaluated at $\mu = \mu_{\text{min}}$ as a function of X , respectively in the solid orange and solid blue line. One observes that $\mu_{\phi}^2(\mu_{\text{min}})$ is much less sensitive to variations at the scale μ_{max} when using the decoupling method. However, there is still quite some fine-tuning necessary even when using the decoupling method, since for a percent-level variation of the high-energy parameters, $|\mu_{\phi}^2|$ changes more than one order of magnitude. To illustrate the robustness of these findings, we explore the behaviour of μ_{ϕ}^2 when varying the model parameters λ_{ϕ} , α , μ_{ϕ}^2 and μ_S^2 . We aim to study how the fine-tuning depends on these parameters, and to show that the choice for our benchmark point is not special. In Fig. 6, the value of μ_{ϕ}^2 at $\mu = \mu_{\text{min}}$ is given as a function of X . In each plot, a different parameter is varied one at a time, while the remaining ones are kept at the same value as in the benchmark point, with $\alpha > 0$ in all plots (negative α yielding qualitatively similar results). Both the decoupling (dashed lines) and non-decoupling (solid lines) results are shown. In the upper-left panel, there is almost no dependence on the value of λ_{ϕ} in the decoupling case (solid lines). Therefore, the three lines overlap almost completely, and only the result for $\lambda_{\phi} = 1.2$ is visible.

We end this section by noting that the large sensitivity at low energy to changes of the parameters of the model at high energy is very different from the analogous sensitivity to the standard logarithmic RG running one has in any theory. Running the SM parameters up to

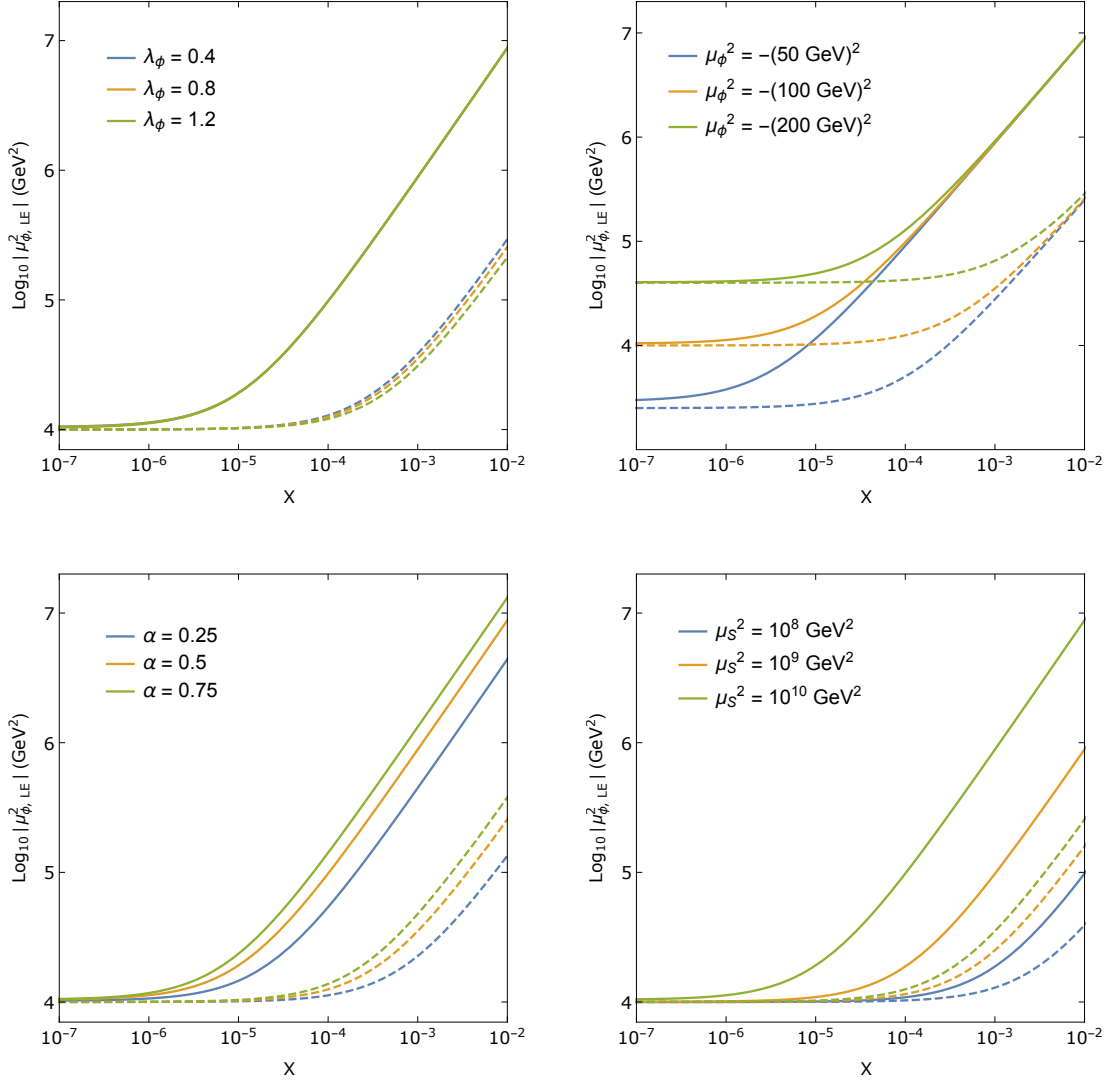


Figure 6: The low-energy value $\mu_{\phi,LE}^2 = \mu_\phi^2(\mu_{\min})$ as a function of X for different model parameter values. The fixed parameters have the value of the benchmark point in Eq. (2.8) with $\alpha > 0$. The solid lines show the results in the non-decoupling case, the dashed lines show the decoupling results.

the GUT scale for instance and then changing the parameters at the GUT scale by a little and then running down, will also generate a substantial difference at low energies. The difference is that in the present case the effects depend quadratically on the large scale as opposed to logarithmically.

4 Alternative implementations of the decoupling method

The decoupling theorem suggests that heavy degrees of freedom cannot be excited, and hence affect the physics, at energies smaller than their masses. However, it is not an exact recipe that specifies at which particular scale the decoupling happens. In the former section, we chose perhaps the simplest prescription [36], where the decoupling scale is fixed completely by the (scalar) particle masses, the exact definition is $\mu_i = m_i e^{-3/4}$. In this section, we elaborate on the fine-tuning and the shape of the potential when considering the different decoupling approaches in refs. [38, 39].

In ref. [38], a formal generalization of the effective potential that we adopted is put forward. The main modification is the appearance of decoupling scales, μ_{m_i} , that are in general different from the mass thresholds m_i , so that the one-loop potential in our model reads

$$V_{\text{dec}}^{(1)} = \frac{1}{4(4\pi)^2} \sum_{i=\phi, S} m_i^4 \left[\log \frac{m_i^2}{\mu_{m_i}^2} + \theta(\mu - \mu_{m_i}) \log \frac{\mu_{m_i}^2}{\mu^2} - \frac{3}{2} \right]. \quad (4.1)$$

One can easily check that for $\mu_{m_i} = m_i e^{-3/4}$ the expression in Eq. (3.1) is recovered. When μ is larger than all the μ_{m_i} , Eq. (4.1) corresponds to the effective potential Eq. (2.4) with no decoupled particles. As the authors in ref. [38] suggest, a reasonable choice for the decoupling scales is $\mu_{m_i} \simeq m_i$, as this improves the validity of the perturbative expansion and follows the reasoning of the decoupling theorem [44, 45]. As mentioned, there is no exact recipe that specifies at which particular scale the decoupling happens, but we find that choosing slightly different scales can have a large effect on the shape of the potential. In order to make our point, we consider two different choices for the decoupling scales to be inserted in Eq. (4.1), namely $\mu_{m_i} = m_i e^{-3/4}$, which is the value of the decoupling scale in the potential (3.1), and $\mu_{m_i} = 1.01 m_i e^{-3/4}$. In the first case, as shown in Fig. 4 (right), we obtained a very good agreement between the tree-level and one-loop potential. In the latter case, despite the decoupling scales being changed at the percent level, the one-loop correction shifts the minimum far away from the tree-level value (more than one order of magnitude), as clearly shown in Fig. 7 (left).¹⁰ This is traced back to the residual log-term (the first term in the squared brackets in Eq. (4.1)), which is multiplied by the large scale $m_S^4 \sim \mu_S^4$. This term gives a large contribution to the potential for $\mu_{m_S} \neq m_S e^{-3/4}$. It is worth mentioning that if one takes decoupling scales $\mu_{m_i} < m_i e^{-3/4}$ (even slightly smaller), the minimum of the one-loop corrected potential disappears because the overall sign of the residual large logarithm in Eq. (4.1) is negative. This applies when $\alpha > 0$, while the situation is reversed when taking $\alpha < 0$, so in that case symmetry breaking will only occur when $\mu_{m_i} < m_i e^{-3/4}$. Hence, just like the non-decoupling approach discussed in Sec. 2.1, the effective potential in Eq. (4.1) leads to a strong dependence of the low-energy physics on the sign of α , i.e. on the interactions involving the high-energy scalar. This behaviour was not

¹⁰The change is not so dramatic if one compares pairs of scales different from $\mu_S e^{-3/4}$, say $\mu_{m_i} = 1.01 m_i$ and $\mu_{m_i} = 1.02 m_i$. However, in that case the VEVs are both much larger than the tree-level result.

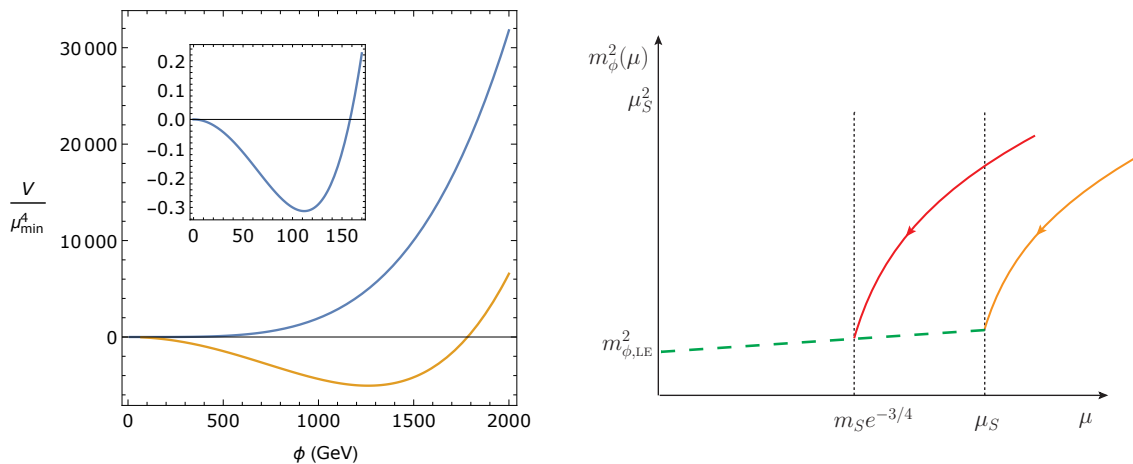


Figure 7: Left: The shape of the potential in the tree-level case at μ_{\min} (blue) and using the decoupling method Eq. (4.1) (orange) for $\alpha = 0.5$. The decoupling scales are set to $\mu_{m_i} = 1.01 \cdot m_i e^{-3/4}$. Right: illustration of the running affected by the heavy scalar S in the decoupling method as in Sec. 3 (red-solid curve) and the EFT method (orange-solid curve), both tuned to give a low-energy ϕ scalar mass. Despite the solid lines just sketching the difference between the two methods, the value for $m_\phi^2(\mu_S)$ resembles our finding in Fig. 4 and, in general, $m_\phi^2(\mu_S)$ is going to be much smaller than μ_S^2 for $\alpha \sim \mathcal{O}(1)$ (though $m_\phi^2(\mu_S) \gg \mu_{\min}^2$).

present when using the decoupling implementation discussed in Sec. 3 according to Eq. (3.1). Our conclusions on the large sensitivity at low energy to changes of the parameters of the model at high energy still hold when considering the more general decoupling approach (4.1), since the RG running of the parameters is only slightly altered compared to the RG running described in Sec. 3.

As a second comparison, we consider the EFT approach as described in ref. [39], which uses the same model Lagrangian as we use (2.1). In this case, a low-energy field theory is explicitly constructed by integrating out the heavy degree of freedom. In doing so, the scalar S does not appear in the effective Lagrangian, though μ_S enters the matching conditions between the effective potentials of the low-energy and high-energy theory. These matching conditions provide the relation between the corresponding masses and couplings (and vacuum energy) in the two theories. In ref. [39], the logarithms vanish when the matching scale is equal to the mass of the heavy scalar μ_S . So this choice minimizes higher-order corrections. Below this scale, the mass parameter m_ϕ runs very modestly, because the heavy degree of freedom is decoupled. Once the smallness of the ϕ -scalar mass in the low-energy theory is imposed, there is little impact on the shape of the potential when one considers one-loop corrections, since the latter are minimized and the heavy degree of freedom does not enter the running. Contrary to the potential in Eq. (4.1), and similarly to the implementation in Eq. (3.1), the shape of the one-loop effective potential stays very close to the tree-level result. However, fine-tuning is still present in this

approach. The fine-tuning can be explicitly noted in the matching condition, where one has to require a very fine cancellation between two large quantities when imposing the lightness of the ϕ scalar mass [39]¹¹

$$m_{\phi,\text{LE}}^2(\mu_S) = m_\phi^2(\mu_S) - \frac{\alpha^2}{8\pi}\mu_S^2, \quad (4.2)$$

where $m_{\phi,\text{LE}}$ is the ϕ -scalar mass in the low-energy theory, whereas m_ϕ is the mass in the high-energy theory. Slightly changing the value of the high-energy parameter m_ϕ at $\mu > \mu_S$, and running it down to $\mu = \mu_S$, would have a significant impact on Eq. (4.2) and it would spoil the lightness of $m_{\phi,\text{LE}}$. When comparing this EFT approach to the decoupling method in Eq. (3.1), one notices that the decoupling scale is different in the two cases: μ_S against $m_S e^{-3/4} \simeq \mu_S/2$. However, the source of the fine-tuning is the same, as the difference between the approaches is only in the energy window where the heavy degree of freedom has an effect, as sketched in Fig. 7 (right). So the amount of fine-tuning that appears in the m_ϕ^2 observable is again very similar in both cases.

To avoid this fine-tuning problem one could supplement the decoupling method or the EFT matching method by the requirement that all parameters of the high-energy theory should be fixed at the decoupling scale of the high-energy scalar. In that way, there will be no large sensitivity to changes of the parameters at the decoupling scale. Running downward will not lead to large changes, while running upward will also not be very dependent on variations of parameters at the decoupling scale (we have numerically checked this statement). The fine-tuning problem that we have addressed arises from running upward beyond the decoupling scale, then modifying the parameters at some higher scale and running down again. In the case of one decoupling scale at high energies, this prescription that all parameters of the high-energy theory should be fixed at the decoupling scale offers a way to avoid the fine-tuning problem. However, when there are multiple decoupling scales, e.g. in case the sum in Eq. (4.1) includes a third particle with a mass that is substantially higher than m_S , there will be large sensitivity to changes of the parameters of the theory at the highest of the decoupling scales (in practice a factor 2 higher will already give rise to a fine-tuning problem). It is very unlikely that if there is new physics, there will be only new particles present in a very narrow range of high-energy scales. So we conclude that the prescription that all parameters of the theory should be fixed at the decoupling scale, will not in general offer a way to avoid the fine-tuning issue we have pointed out in this paper.

5 Conclusion

In this paper we have carried out an analysis of the hierarchy problem from the viewpoint of the effective potential. Our study does not propose any solution to the hierarchy problem, rather it aims to show that this issue is present in the extraction of the observables from the

¹¹We adapted the expression to our different notation for the couplings and mass parameters.

effective potential, even when using a decoupling approach. For this purpose we have mainly concentrated on the decoupling method of [36], which freezes the effect of heavy particles on the running at low energies. Working at the one-loop level, and within a simple two-scalar theory, we disentangled the effects of the high-energy degree of freedom on the shape of the potential and on the fine-tuning of the model parameters. We find that while the decoupling method leads to an acceptable and convergent effective potential, the method does not solve the fine-tuning problem that is inherent to the hierarchy problem of multiple-scale theories. Compared to the non-decoupling approach, the amount of fine-tuning is reduced. Nevertheless, the mass of the low-energy scalar turns out to be still very sensitive to small changes of the parameters at the scale of the high-energy sector.

We considered two other implementations of the decoupling method which lead to different conclusions on the impact of quantum corrections on the shape of the potential, in particular on the VEV of the low-energy scalar field. For the decoupling potential in Eq. (4.1), we find that small deviations from the “reference” decoupling scale $\mu_S e^{-3/4}$ make the minimum shift far away from the tree-level value if $\mu_{m_i} > m_i e^{-3/4}$, whereas the minimum is absent whenever $\mu_{m_i} < m_i e^{-3/4}$, when $\alpha > 0$. The situation is reversed when negative values for α are used. Therefore, the decoupling method outlined in Eq. (4.1) reintroduces the dependence of the shape of the potential, and the existence of a non-trivial minimum, on the sign of the coupling α (as it was for the non-decoupling approach described in Sec. 2). On the contrary, the EFT approach guarantees fairly small loop corrections for the low-energy parameters at scales below the decoupling scale (which is set to the high-scale mass parameter μ_S). The fine-tuning problem is very similar in the different implementations, however. In case there is only one decoupling scale at large energy, one can avoid the fine-tuning by requiring that all parameters of the high-energy theory should be specified at the decoupling scale. But in the case of two or more high-energy decoupling scales the fine-tuning problem resurfaces. There appears to be no straightforward way to adjust the decoupling method to avoid this problem.

Acknowledgements

The work of S.B. is supported by the Swiss National Science Foundation (SNF) under the Ambizione grant PZ00P2_185783. S.B. is grateful to the FSE fellowship program at the University of Groningen where this work was started. The work of R.P. is supported by the NWO programme “Higgs as a probe and portal”. The authors thank Bogumiła Świeżewska for useful discussions.

References

- [1] J. McDonald, “Gauge singlet scalars as cold dark matter,” *Phys. Rev. D*, vol. 50, pp. 3637–3649, 1994, hep-ph/0702143.
- [2] C. Burgess, M. Pospelov, and T. ter Veldhuis, “The Minimal model of nonbaryonic dark matter: A Singlet scalar,” *Nucl. Phys. B*, vol. 619, pp. 709–728, 2001, hep-ph/0011335.
- [3] R. M. Schabinger and J. D. Wells, “A Minimal spontaneously broken hidden sector and its impact on Higgs boson physics at the large hadron collider,” *Phys. Rev. D*, vol. 72, p. 093007, 2005, hep-ph/0509209.
- [4] L. Feng, S. Profumo, and L. Ubaldi, “Closing in on singlet scalar dark matter: LUX, invisible Higgs decays and gamma-ray lines,” *JHEP*, vol. 03, p. 045, 2015, 1412.1105.
- [5] M. Fukugita and T. Yanagida, “Baryogenesis Without Grand Unification,” *Phys. Lett. B*, vol. 174, pp. 45–47, 1986.
- [6] J. R. Espinosa and M. Quiros, “Novel Effects in Electroweak Breaking from a Hidden Sector,” *Phys. Rev. D*, vol. 76, p. 076004, 2007, hep-ph/0701145.
- [7] C. Englert, J. Jaeckel, V. Khoze, and M. Spannowsky, “Emergence of the Electroweak Scale through the Higgs Portal,” *JHEP*, vol. 04, p. 060, 2013, 1301.4224.
- [8] A. Farzinnia, H.-J. He, and J. Ren, “Natural Electroweak Symmetry Breaking from Scale Invariant Higgs Mechanism,” *Phys. Lett. B*, vol. 727, pp. 141–150, 2013, 1308.0295.
- [9] V. V. Khoze, “Inflation and Dark Matter in the Higgs Portal of Classically Scale Invariant Standard Model,” *JHEP*, vol. 11, p. 215, 2013, 1308.6338.
- [10] E. Gildener, “Gauge Symmetry Hierarchies,” *Phys. Rev. D*, vol. 14, p. 1667, 1976.
- [11] L. Susskind, “Dynamics of Spontaneous Symmetry Breaking in the Weinberg-Salam Theory,” *Phys. Rev. D*, vol. 20, pp. 2619–2625, 1979.
- [12] G. ’t Hooft, “Naturalness, chiral symmetry, and spontaneous chiral symmetry breaking,” *NATO Sci. Ser. B*, vol. 59, pp. 135–157, 1980.
- [13] S. Weinberg, “Gauge Hierarchies,” *Phys. Lett. B*, vol. 82, pp. 387–391, 1979.
- [14] M. Veltman, “The Infrared - Ultraviolet Connection,” *Acta Phys. Polon. B*, vol. 12, p. 437, 1981.
- [15] G. F. Giudice, “Naturalness after LHC8,” *PoS*, vol. EPS-HEP2013, p. 163, 2013, 1307.7879.

- [16] M. Shaposhnikov, “Is there a new physics between electroweak and Planck scales?,” in *Astroparticle Physics: Current Issues, 2007 (APCI07)*, 8 2007, 0708.3550.
- [17] J. Wess and B. Zumino, “A Lagrangian Model Invariant Under Supergauge Transformations,” *Phys. Lett. B*, vol. 49, p. 52, 1974.
- [18] J. Iliopoulos and B. Zumino, “Broken Supergauge Symmetry and Renormalization,” *Nucl. Phys. B*, vol. 76, p. 310, 1974.
- [19] R. K. Kaul, “Gauge Hierarchy in a Supersymmetric Model,” *Phys. Lett. B*, vol. 109, pp. 19–24, 1982.
- [20] S. P. Martin, *A Supersymmetry primer*, vol. 21, pp. 1–153. 2010, hep-ph/9709356.
- [21] D. B. Kaplan, H. Georgi, and S. Dimopoulos, “Composite Higgs Scalars,” *Phys. Lett. B*, vol. 136, pp. 187–190, 1984.
- [22] M. J. Dugan, H. Georgi, and D. B. Kaplan, “Anatomy of a Composite Higgs Model,” *Nucl. Phys. B*, vol. 254, pp. 299–326, 1985.
- [23] B. Bellazzini, C. Csáki, and J. Serra, “Composite Higgses,” *Eur. Phys. J. C*, vol. 74, no. 5, p. 2766, 2014, 1401.2457.
- [24] N. Arkani-Hamed, S. Dimopoulos, and G. Dvali, “Phenomenology, astrophysics and cosmology of theories with submillimeter dimensions and TeV scale quantum gravity,” *Phys. Rev. D*, vol. 59, p. 086004, 1999, hep-ph/9807344.
- [25] N. Arkani-Hamed, S. Dimopoulos, and G. Dvali, “The Hierarchy problem and new dimensions at a millimeter,” *Phys. Lett. B*, vol. 429, pp. 263–272, 1998, hep-ph/9803315.
- [26] L. Randall and R. Sundrum, “A Large mass hierarchy from a small extra dimension,” *Phys. Rev. Lett.*, vol. 83, pp. 3370–3373, 1999, hep-ph/9905221.
- [27] J. L. Feng, “Naturalness and the Status of Supersymmetry,” *Ann. Rev. Nucl. Part. Sci.*, vol. 63, pp. 351–382, 2013, 1302.6587.
- [28] J. D. Wells, “The Utility of Naturalness, and how its Application to Quantum Electrodynamics envisages the Standard Model and Higgs Boson,” *Stud. Hist. Phil. Sci. B*, vol. 49, pp. 102–108, 2015, 1305.3434.
- [29] J. Barnard and M. White, “Collider constraints on tuning in composite Higgs models,” *JHEP*, vol. 10, p. 072, 2015, 1507.02332.
- [30] M. Quiros, “Finite temperature field theory and phase transitions,” in *ICTP Summer School in High-Energy Physics and Cosmology*, pp. 187–259, 1 1999, hep-ph/9901312.

- [31] M. B. Einhorn and D. Jones, “A new renormalization group approach to multiscale problems,” *Nucl. Phys. B*, vol. 230, pp. 261–272, 1984.
- [32] C. Ford, “Multiscale renormalization group improvement of the effective potential,” *Phys. Rev. D*, vol. 50, pp. 7531–7537, 1994, hep-th/9404085.
- [33] C. Ford and C. Wiesendanger, “Multiscale renormalization,” *Phys. Lett. B*, vol. 398, pp. 342–346, 1997, hep-th/9612193.
- [34] M. Bando, T. Kugo, N. Maekawa, and H. Nakano, “Improving the effective potential: Multimass scale case,” *Prog. Theor. Phys.*, vol. 90, pp. 405–418, 1993, hep-ph/9210229.
- [35] M. Bando, T. Kugo, N. Maekawa, and H. Nakano, “Improving the effective potential,” *Phys. Lett. B*, vol. 301, pp. 83–89, 1993, hep-ph/9210228.
- [36] J. Casas, V. Di Clemente, and M. Quiros, “The Effective potential in the presence of several mass scales,” *Nucl. Phys. B*, vol. 553, pp. 511–530, 1999, hep-ph/9809275.
- [37] L. Chataignier, T. Prokopec, M. G. Schmidt, and B. Swiezewska, “Single-scale Renormalisation Group Improvement of Multi-scale Effective Potentials,” *JHEP*, vol. 03, p. 014, 2018, 1801.05258.
- [38] J. Casas, V. Di Clemente, and M. Quiros, “The Standard model instability and the scale of new physics,” *Nucl. Phys. B*, vol. 581, pp. 61–72, 2000, hep-ph/0002205.
- [39] I. Masina, G. Nardini, and M. Quiros, “Electroweak vacuum stability and finite quadratic radiative corrections,” *Phys. Rev. D*, vol. 92, no. 3, p. 035003, 2015, 1502.06525.
- [40] A. V. Manohar and E. Nardoni, “Renormalization Group Improvement of the Effective Potential: an EFT Approach,” 10 2020, 2010.15806.
- [41] K. Kannike, “Vacuum Stability Conditions From Copositivity Criteria,” *Eur. Phys. J. C*, vol. 72, p. 2093, 2012, 1205.3781.
- [42] H. Okane, “Construction of a renormalization group improved effective potential in a two real scalar system,” *PTEP*, vol. 2019, no. 4, p. 043B03, 2019, 1901.05200.
- [43] E. J. Weinberg and A.-q. Wu, “Understanding complex perturbative effective potentials,” *Phys. Rev. D*, vol. 36, p. 2474, 1987.
- [44] K. Symanzik, “Infrared singularities and small distance behavior analysis,” *Commun. Math. Phys.*, vol. 34, pp. 7–36, 1973.
- [45] T. Appelquist and J. Carazzone, “Infrared Singularities and Massive Fields,” *Phys. Rev. D*, vol. 11, p. 2856, 1975.